

Temperature dependence of the ESR spectrum of $\text{NiSnCl}_6 \cdot 6\text{H}_2\text{O}$ [†]

Y. Ajiro,* S. A. Friedberg, and N. S. VanderVen

Physics Department, Carnegie-Mellon University, Pittsburgh, Pennsylvania 15213

(Received 10 February 1975)

The electron-spin-resonance spectrum of single-crystal $\text{NiSnCl}_6 \cdot 6\text{H}_2\text{O}$ has been measured at X band at temperatures between 4.2 and 370 K. The results are consistent with low-temperature magnetic and thermal measurements that indicate a singlet ground state for the $\text{Ni}(\text{H}_2\text{O})_6^{++}$ complex. The data are described by the spin Hamiltonian $\mathcal{H} = \mu_B [g_{\parallel} H_z S_z + g_{\perp} (H_x S_x + H_y S_y)] + D(S_z^2 - 2/3)$ with $S = 1$. At $T = 4.2$ K, $D = 0.458 \pm 0.004$ cm⁻¹, but it decreases rapidly with increasing temperature, passing through zero at 338 ± 5 K and becoming negative at higher temperatures. Above 77 K, $g_{\parallel} \approx g_{\perp} = 2.33 \pm 0.04$. At 77 K and below, $g_{\parallel} = 2.26 \pm 0.02$, $g_{\perp} = 2.18 \pm 0.02$. Linewidth measurements below 300 K indicate contributions from spin-lattice relaxation and from both isotropic and anisotropic exchange. Linewidth measurements in the vicinity of $D = 0$ exhibit narrowing due to vanishing of the isotropic exchange contribution and broadening by cross relaxation.

I. INTRODUCTION

Recent low-temperature thermal and magnetic measurements¹ have established that in $\text{NiSnCl}_6 \cdot 6\text{H}_2\text{O}$ the $\text{Ni}(\text{H}_2\text{O})_6^{++}$ complex has a non-degenerate (singlet) ground state. In the octahedral electric field of the water molecules the ground state of the Ni^{++} ion is an orbital singlet, separated by about 10 000 cm⁻¹ from higher orbital levels. This lowest orbital level is a spin triplet ($S = 1$) that in a cubic electric field would be triply degenerate. Fields of lower symmetry reduce the degeneracy; in particular the addition of a small axial (trigonal) distortion splits the triplet into a doublet and a singlet. In a magnetic field the ground state of such an axially distorted complex is described by the spin Hamiltonian²

$$\mathcal{H} = \mu_B [g_{\parallel} H_z S_z + g_{\perp} (H_x S_x + H_y S_y)] + D(S_z^2 - \frac{2}{3}), \quad (1)$$

where the \hat{z} direction is along the axis of the distortion. Experimentally g is found to be nearly isotropic. In zero magnetic field, for $D > 0$, the ground state is a singlet separated by an energy D from the excited doublet.

Systems in which there is one axially distorted Ni^{++} complex per unit cell with a singlet ground state are of interest for several reasons. One is the possibility of observing cooling upon adiabatic demagnetization.^{3,4} Another is the possibility of observing "subcritical" interactions^{5,6} among the Ni^{++} ions such that there is no long-range order at any temperature in zero magnetic field. These effects are discussed in some detail in an earlier paper,¹ in which it was pointed out that nickel chlorostannate is the first salt to be studied in which there is only one Ni^{++} complex per unit cell

with an axial distortion leading to a singlet ground state.

Although $\text{NiSnCl}_6 \cdot 6\text{H}_2\text{O}$ is the prototype of a family of isostructural trigonal crystals, it had not, except for the structural determination,⁷ been studied until quite recently. The most extensively studied salt (whose structure is in fact inferred from that of the $\text{NiSnCl}_6 \cdot 6\text{H}_2\text{O}$) is $\text{NiSiF}_6 \cdot 6\text{H}_2\text{O}$, for which magneto-optic^{8,9} and paramagnetic-resonance¹⁰ measurements have determined that the crystal-field distortion is purely axial with $D < 0$, and that there is a pronounced temperature dependence of D .

Magnetic anisotropy measurements¹¹ on the chlorostannate had suggested that D was also negative at low temperatures but that the temperature dependence was weak. Recent measurements at low temperatures of the magnetic susceptibility, isothermal magnetization, and heat capacity,¹ and the work to be reported in this paper, do not support these conclusions.

This paper describes paramagnetic resonance measurements on single-crystal $\text{NiSnCl}_6 \cdot 6\text{H}_2\text{O}$ at X band between 4.2 and 370 K. The spectrum has been studied in detail as a function of temperature and of crystal orientation. The details of the experiments are described in Sec. II; in Sec. III the results are presented and discussed.

II. EXPERIMENTAL

The homodyne paramagnetic resonance spectrometer was conventional in most respects except that a ferrite circulator replaced the usual magic-tee bridge. The klystron frequency was locked by standard FM methods to the half-wave rectangular (TE_{101}) sample cavity, whose reflection coefficient could be varied with a coupler of the type described

by Gordon.¹² Audio-frequency field modulation and phase-sensitive detection gave a recorder display of $d\chi''/dH$.

Below room temperature, data were taken at fixed points of 4.2, 77, 195, and 273 K. Temperatures above 300 K were obtained by enclosing the cavity in a small oven consisting of a close-fitting brass can with external heater windings. A copper-constantan thermocouple embedded in the cavity wall was used to measure temperatures in this range, which were controlled to ± 1 K during an experimental run.

Small single crystals were prepared as described by Myers *et al.*¹ They were mounted on the cavity wall with GE 7031 lacquer, and given a light coating of silicone vacuum grease for protection. The trigonal axis of a crystal was determined by inspection. The field could be oriented along the trigonal axis to within $\pm 2^\circ$.

In studying the angular dependence of the spectrum, the sample was mounted with the trigonal axis horizontal and the microwave field H_1 vertical. The field H_0 was horizontal, and could be oriented by rotating the magnet about a vertical axis. This arrangement does not provide the optimum configuration for observing the transitions when H_0 is perpendicular to the trigonal axis, for which the maximum transition probability occurs when H_1 is parallel to the trigonal axis. This is not a serious problem unless the Zeeman energy is much less than the crystal-field splitting, and it caused no difficulty in our measurements, for which the signal intensity was always sufficient.

III. RESULTS AND DISCUSSION

A. Angular dependence of resonance transitions

Because the crystal field and Zeeman energies are comparable, analysis of the data requires that the spin Hamiltonian be treated exactly. In units of D , Eq. (1) may be rewritten as

$$\mathcal{H} = h_{\parallel} \cos\theta S_z + h_{\perp} \sin\theta S_x + (S_z^2 - \frac{3}{5}), \quad (2)$$

where $h_{\parallel} \equiv g_{\parallel} \mu_B H/D$, $h_{\perp} \equiv g_{\perp} \mu_B H/D$, and θ is the angle between the external field H and the crystal-field axis. With the field applied parallel and perpendicular to the axis the eigenvalues in units of D are, respectively,

$$\epsilon_{\parallel} = -\frac{2}{3}, \frac{1}{3} \pm h_{\parallel}, \quad (3)$$

$$\epsilon_{\perp} = \frac{1}{3}, -\frac{1}{6} \pm \frac{1}{2}(1 + 4h_{\perp}^2)^{1/2}. \quad (4)$$

These are shown in Fig. 1, with an indication of the allowed and forbidden transitions in a resonance experiment designed to detect $\Delta M_s = \pm 1$.

For arbitrary angles the secular determinant cannot be factored, but if $g_{\parallel} = g_{\perp}$ the resonance fields for any orientation may be found by a tech-

nique developed for the analysis of triplet-state ESR spectra.^{13, 14} Taking $h_{\parallel} = h_{\perp} = h$, one obtains the eigenvalues as the roots of the secular equation

$$\epsilon^3 - \epsilon(h^2 + \frac{1}{3}) + h^2(\frac{1}{3} - \cos^2\theta) + \frac{2}{27} = 0. \quad (5)$$

Experimentally the microwave quantum is fixed ($\approx 0.3 \text{ cm}^{-1}$) while the external field is varied. Resonance absorption is energetically possible if

$$\epsilon_2 - \epsilon_1 = \delta, \quad (6)$$

where ϵ_2 and ϵ_1 are any two roots of Eq. (5) and $\delta \equiv \hbar\omega/D$. Upon combining Eqs. (5) and (6), the possible orientations for which resonance may occur in a field h are found to be

$$\cos^2\theta = (27h)^{-1} [(2 + 9h^2) \pm (3\delta^2 - 3h^2 - 1)(-3\delta^2 + 12h^2 + 4)^{1/2}]. \quad (7)$$

If the right-hand side is plotted with h as ordinate, the resonance fields for a given orientation are given by the intercepts with vertical lines representing fixed values of $\cos^2\theta$. The rotation diagrams thus obtained give all transitions that are energetically possible, without regard for their relative strength.

These rotation diagrams vary in character, depending on the magnitude of δ . Three cases may be distinguished.

(i) $\delta < 1$, illustrated in Fig. 2 for $\delta = 0.5$. The microwave quantum is less than D , giving only one transition for H_{\perp} . The rotation diagram then has only two branches. The single transition W_{23} for H_{\perp} lies on the same branch as the forbidden transition W_{-+} for H_{\parallel} . The semiclosed branch is the locus of the two transitions corresponding to the two W_{0-} transitions for H_{\parallel} . As the field is rotated away from the axis these two transitions merge, become degenerate, and are then no longer energetically allowed.

For $\delta > 1$ the microwave quantum is greater than D , giving two allowed transitions for H_{\perp} . The rotation diagram has three branches, giving in general three allowed transitions at intermediate angles. There are two types of rotation diagram for $\delta > 1$, but in both cases the high-field allowed transition W_{0-} for H_{\parallel} and the low-field allowed transition W_{12} for H_{\perp} lie on the same branch.

(ii) $1 < \delta < 2$, illustrated in Fig. 2 for $\delta = 1.5$. Here the forbidden transition W_{-+} for H_{\parallel} and the high-field allowed transition W_{23} for H_{\perp} lie on one branch. The other branch connects the allowed transition W_{0+} for H_{\parallel} with the forbidden transition W_{13} for H_{\perp} .

(iii) $\delta > 2$, illustrated in Fig. 2 for $\delta = 1.5$. Now the allowed transitions W_{0+} and W_{23} lie on the same branch, while the forbidden transitions W_{-+} and

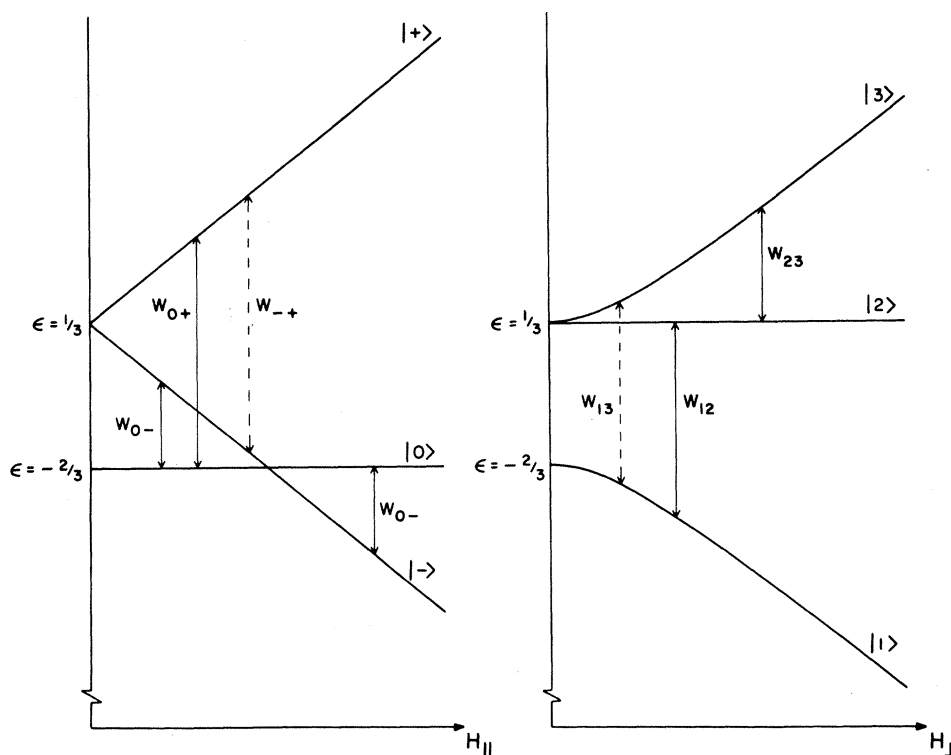


FIG. 1. Energy levels of a singlet-ground-state system ($S=1$, $D < 0$) with the external field parallel (H_{\parallel}) and perpendicular (H_{\perp}) to the trigonal axis. Allowed and forbidden transitions are indicated.

W_{23} lie on the other branch.

Experimental rotation diagrams for $T=4.2$, 195, and 273 K are shown in Figs. 3–5, respectively. These diagrams are not essential to the determination of D , g_{\parallel} , and g_{\perp} , which are obtained entirely from data at $\theta=0$ and $\frac{1}{2}\pi$, but they are important for an understanding of the angular dependence of the linewidth, to be discussed presently. Also shown in these figures are theoretical curves calculated from Eq. (7), using the values of D and g_{\parallel} inferred from the parallel-field data.

B. Temperature dependence of D and g

The low-temperature susceptibility measurements have established that D is positive in nickel chlorostannate. We find that the magnitude of D is 0.458 cm^{-1} at 4.2 K and decreases rapidly with increasing temperature. In the vicinity of room temperature the variation is linear. D passes through zero at $338 \pm 5 \text{ K}$ and assumes negative values above that point, continuing to vary linearly up to the highest temperature of our measurements.

The temperature dependence is shown in Fig. 6, along with the temperature dependence in nickel fluosilicate.¹⁰ The two curves are nearly identical, save for a relative displacement such that in the fluosilicate D is always negative. Figure 7 shows the detailed temperature variation of D in the chlorostannate in the region of the zero crossing

where the temperature dependence is linear, given by

$$D(T) \approx -2(T - 338) \times 10^{-3} \text{ cm}^{-1}. \quad (8)$$

We find $g_{\parallel} \approx 2.30$, independent of temperature within the experimental error. This is in good agreement with values obtained for Ni^{2+} in similar salts.¹⁰ Above 150 K we find $g_{\parallel} \approx g_{\perp}$. At 77 and 4.2 K there is some evidence that g_{\parallel} differs from g_{\perp} ; the results are summarized in Table I. Below about 150 K the microwave quantum is less than D at X band frequencies. Under these conditions, with only one resonance transition for H_{\perp} , values for D and g_{\parallel} are inferred from data for H_{\parallel} , while g_{\perp} is obtained from the appropriate combination of parallel- and perpendicular-field data. Above 150 K, when the microwave quantum is greater than D , there are two resonances for H_{\perp} , permitting a determination of g_{\perp} and of D entirely from perpendicular-field data. Above 150 K we find $g_{\parallel} = g_{\perp}$ and excellent agreement between the two independent determinations of D . We plan to carry out low-temperature measurements at K band, for which the microwave quantum is greater than D down to 4.2 K and probably well below. We do not now understand the origin of the low-temperature difference between g_{\parallel} and g_{\perp} . In any event the difference, if real, is rather small.

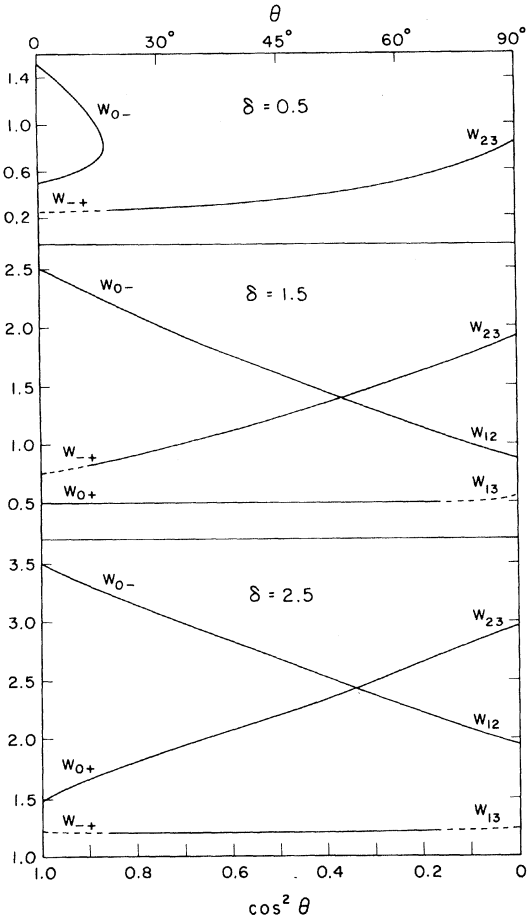


FIG. 2. Resonance rotation diagrams determined from Eq. (7) for various values of $\delta (= \hbar\omega/D)$. The labeling of the transitions corresponds to that of Fig. 1.

C. Linewidth

1. Temperature dependence

The temperature dependence of the linewidth (FWHM) with the applied field parallel to the trigonal axis is shown in Fig. 8. Apart from the anomalous behavior in the region near the temperature for which $D=0$, the linewidth increases monotonically with increasing field, suggesting that at high temperatures there is appreciable lifetime broadening by fast spin-lattice relaxation. In Fig. 9 these results are shown in slightly different form, omitting the data between 330 and 350 K and plotting the average of the linewidths of the high- and low-field transitions. Except for the anomaly in the vicinity of 338 K (where $D=0$) the data can be described quite well by a temperature dependence of the form

$$\Delta H_{\parallel} = a + bT^2, \quad (9)$$

with $a = 325$ Oe and $b = 2.5 \times 10^{-3}$ Oe K $^{-2}$.

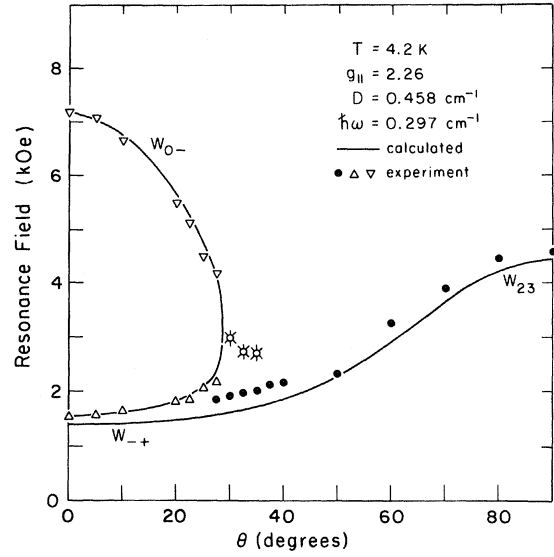


FIG. 3. Experimental resonance rotation diagram in $\text{NiSnCl}_6 \cdot 6\text{H}_2\text{O}$ for $T = 4.2$ K. Low-field and high-field W_{0-} transitions are indicated with Δ and ∇ , respectively. Transitions marked by open asterisks are unresolved.

The term quadratic in the temperature can be attributed to spin-lattice relaxation by a two-phonon Raman process. Well above the Debye temperature Θ_D the approximate temperature dependence of this contribution is given by¹⁵

$$\frac{g\mu_B}{h} \Delta H \approx \frac{9k^7}{10\pi^3 \hbar^7} \frac{\Theta_D^5}{\rho^2 v^{10}} \left(V_{(2)}^2 + \frac{V_{(1)}}{\Delta^2} T^2 \right), \quad (10)$$

where $V_{(1)}$ and $V_{(2)}$ are the coefficients, respectively, of the linear and quadratic terms in an expansion of the crystal potential in powers of the

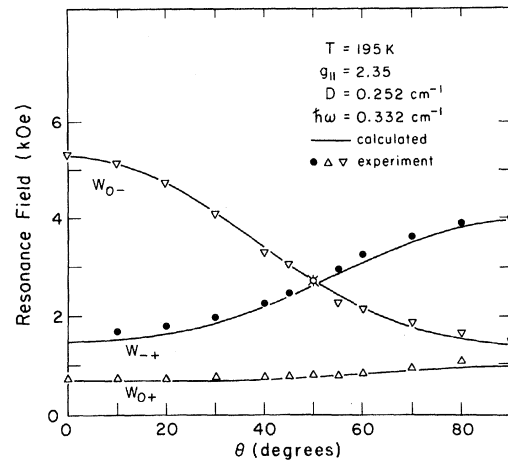


FIG. 4. Experimental rotation diagram for $T = 195$ K. Transitions marked by open asterisks are unresolved.

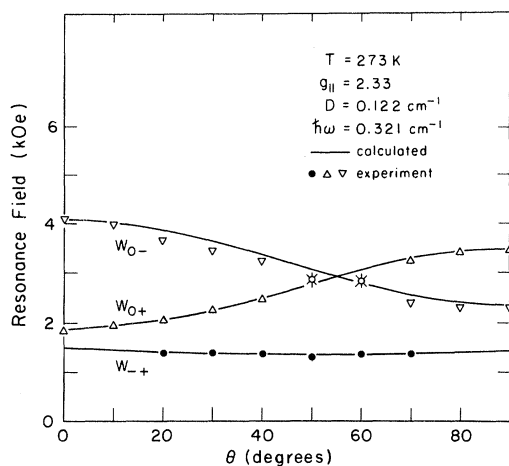


FIG. 5. Experimental rotation diagram for $T=273$ K. Transitions marked by open asterisks are unresolved.

strain, and Δ is the energy of the excited state to which virtual transitions occur. A value of $\Theta_D \approx 80$ K is obtained from the lattice specific heat; a splitting $\Delta \approx 9000$ cm^{-1} is assumed, based on optical absorption measurements in the fluosilicate.¹⁶ Taking $V_{(1)} = V_{(2)} = \Delta$, and $v = 5 \times 10^5$ cm/sec , we obtain an estimate for b of 1.2×10^{-3} Oe K^{-2} , in good agreement with the experimental value in view of the approximations involved.

The temperature-independent term is due to a combination of spin-spin broadening mechanisms. These include dipolar coupling, anisotropic exchange, and, in the presence of a crystalline-field splitting, isotropic exchange. Assuming only

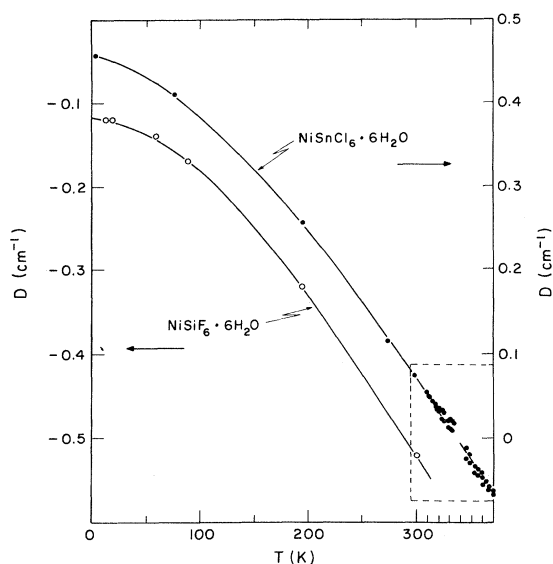


FIG. 6. Axial crystal-field splitting D vs T for $\text{NiSnCl}_6 \cdot 6\text{H}_2\text{O}$ and $\text{NiSiF}_6 \cdot 6\text{H}_2\text{O}$.

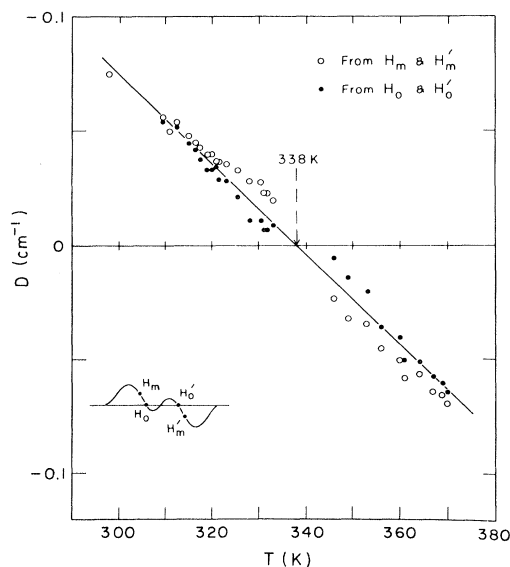


FIG. 7. Detailed temperature dependence of D for $\text{NiSnCl}_6 \cdot 6\text{H}_2\text{O}$ in the vicinity of the zero crossing at $T=338$ K. Two methods of determining the line position are indicated.

dipolar coupling and isotropic exchange, Ishiguro, Kambe, and Usui¹⁷ analyzed the room-temperature linewidth data for nickel fluosilicate measured by Holden, Kittel, and Yager.¹⁸ They concluded that the isotropic exchange contribution was much larger than the dipolar contribution, but that the inferred exchange constant was about 50% greater than that obtained from susceptibility and magneto-optical rotation measurements. This discrepancy was adduced as evidence for an additional contribution due to anisotropic exchange that would contribute to the second moment but would not, if of pseudodipolar type, affect the susceptibility. However, as we have seen in the chlorostannate, room-temperature linewidths contain appreciable

TABLE I. D , $g_{||}$, and g_{\perp} for $\text{NiSnCl}_6 \cdot 6\text{H}_2\text{O}$. When two values of D are indicated, the first is derived from parallel-field data, the second from perpendicular-field data.

T (K)	$g_{ }$	g_{\perp}	D (cm^{-1})
4.2	2.26 ± 0.02	2.19 ± 0.02	0.458 ± 0.004
77	2.27 ± 0.02	2.17 ± 0.02	0.403 ± 0.004
195	2.35 ± 0.03	2.38 ± 0.03	0.252 ± 0.003 0.252 ± 0.003
273	2.33 ± 0.04	2.35 ± 0.04	0.252 ± 0.003 0.252 ± 0.003
298	2.28 ± 0.04	2.30 ± 0.04	0.078 ± 0.001 0.079 ± 0.001

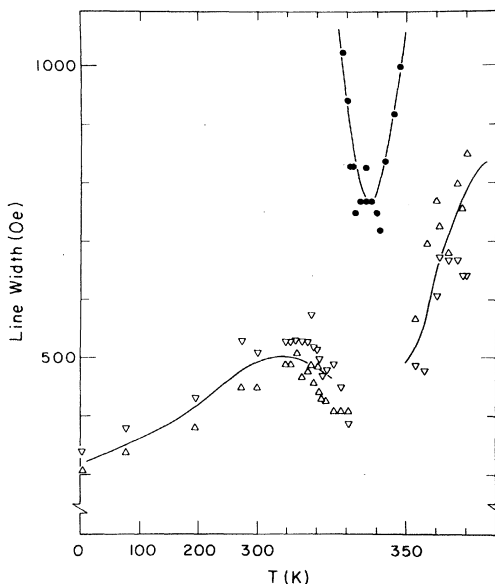


FIG. 8. Temperature dependence of the linewidth in $\text{NiSnCl}_6 \cdot 6\text{H}_2\text{O}$ for H parallel to the trigonal axis.

spin-lattice contributions, and spin-spin broadening should be inferred from low-temperature measurements. Ishiguro *et al.* remarked on this difficulty, but were forced to analyze the room-temperature data since low-temperature linewidth data had not then been published. In view of this, the room-temperature linewidth data cannot be taken as evidence, *per se*, of anisotropic exchange in the fluosilicate. From careful measurements of the low-temperature dependence of the position and shape of the ESR lines, Svare and Seidel¹⁹ have concluded that in the fluosilicate the exchange interaction is isotropic and ferromagnetic, with a value $A = -3.9 \times 10^{-18}$ erg.

In the chlorostannate we measure low-temperature linewidths of 325 Oe for H_{\parallel} and 440 Oe for H_{\perp} . The calculations of Ishiguro *et al.* may be extended to include anisotropic exchange of the pseudodipolar type. Assuming that the nickel ions form a simple cubic structure of lattice constant d , and including only nearest-neighbor interactions, we find the second moment to be

$$\begin{aligned} \langle (\Delta H_{\parallel})^2 \rangle &= \frac{6A^2}{g_{\parallel}^2 \mu_B^2} + 3.13 \left(\frac{g_{\parallel}^2 \mu_B^2}{d^6} + \frac{B^2}{g_{\parallel}^2 \mu_B^2} \right), \\ \langle (\Delta H_{\perp})^2 \rangle &= \frac{6A^2}{g_{\perp}^2 \mu_B^2} + 6.50 \left(\frac{g_{\perp}^2 \mu_B^2}{d^6} + \frac{B^2}{g_{\perp}^2 \mu_B^2} \right). \end{aligned} \quad (11)$$

The first term is due to isotropic exchange; the second and third terms are, respectively, the dipolar and pseudodipolar contributions. For $d = 7.09 \text{ \AA}$ the rms dipolar contributions are 158 Oe for H_{\parallel} and 227 Oe for H_{\perp} , indicating that exchange

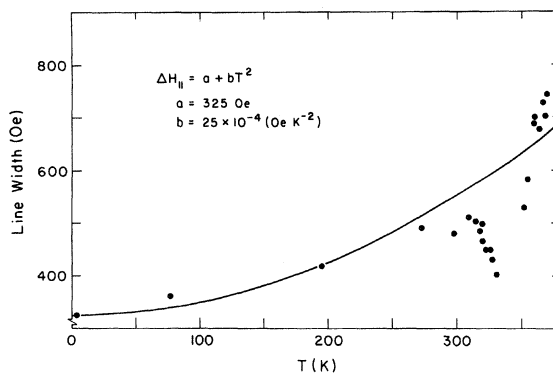


FIG. 9. Average linewidth of the high- and low-field W_{0-} transitions in $\text{NiSnCl}_6 \cdot 6\text{H}_2\text{O}$ with H parallel to the trigonal axis.

is a significant contribution. The estimated exchange constants are $|A| = 1.3 \times 10^{-18}$ erg and $|B| = 3.2 \times 10^{-19}$ erg. Treating the net interaction in a molecular field approximation, Myers *et al.* estimated the coupling constant n to be -0.02 mole/emu. Attributing this exclusively to isotropic exchange would yield $|A| = 1.3 \times 10^{-19}$ erg.

One should not take too seriously our estimate of exchange constants based on Eq. (11). These apply strictly only in the limit $g\mu_B H \ll D$, a condition obviously not met in our experiments. Expressions for the second moment in the presence of both types of exchange have not been obtained when the Zeeman energy and crystal-field splitting are comparable.

As the crystal-field splitting goes to zero, the isotropic exchange contribution to the second moment vanishes, and one might expect to observe line narrowing under conditions for which $D \approx 0$. Such was not the case in the fluosilicate, for which Walsh²⁰ was able to change the sign of D by the application of pressure. He observed that the line broadened monotonically as D , negative at atmospheric pressure, passed through zero and became positive. No anomalies were observed in the vicinity of $D = 0$. The explanation was that, although the isotropic exchange contribution disappears, the contributions of both dipolar and pseudodipolar coupling increase as the crystal field goes to zero and all spins become equivalent. Estimates of the dipolar contribution indicated the necessity for a certain amount of anisotropic exchange. It is somewhat surprising, however, that the narrowing and broadening effects exactly compensate.

In the chlorostannate, where D can be made to vanish by temperature changes alone, the situation is quite different, as may be seen in Figs. 8 and 9. For temperatures near 338 K, but still sufficiently

far away that the high- and low-field resonances are resolved, the line is clearly narrower than the width given by Eq. (9). This narrowing is presumably due to the vanishing of the isotropic exchange contribution. Our ability to observe this narrowing in the chlorostannate is due to the comparatively narrower line, permitting us to follow the resolved resonances much closer in toward $D=0$ than could Walsh in the fluosilicate, where the lines are three times as broad. Still closer to 338 K the lines overlap and only the apparent width of the composite line can be observed.

At $D=0$, where the lines exactly coincide, the width can again be measured, and is found to lie well above the value given by Eq. (7). We believe that the excess broadening is due to cross relaxation²¹ as the two resonance curves (W_{0-} , W_{0+} transitions) overlap. The probability of energy transfer between the high- and low-field resonant spins increases as the line splitting becomes small compared with the spin-spin interaction, leading to a contribution to the line width given by

$$\Delta H_{\text{cross}} = \langle \langle (\Delta H)^2 \rangle \rangle^{1/2} \exp\left(\frac{-D^2(T)}{g^2 \mu_B \langle \langle (\Delta H)^2 \rangle \rangle}\right), \quad (12)$$

where $\langle \langle (\Delta H)^2 \rangle \rangle^{1/2}$ is the linewidth due to spin-spin interactions. The spin-spin contribution is itself a function of temperature, but a reasonable fit to the data can be made by taking it to be about 300 Oe, as suggested by the data of Fig. 8.

2. Angular dependence

Further confirmation of cross-relaxation broadening is seen in the angular dependence of the linewidth, shown in Figs. 10–12 for $T=4.2$, 195, and

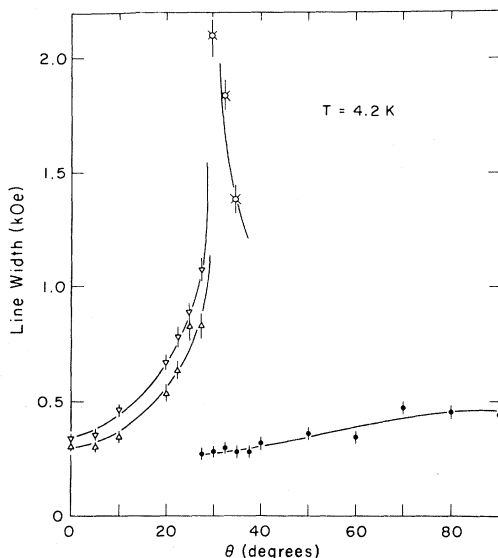


FIG. 10. Linewidth vs θ in $\text{NiSnCl}_6 \cdot 6\text{H}_2\text{O}$ for $T=4.2$ K.

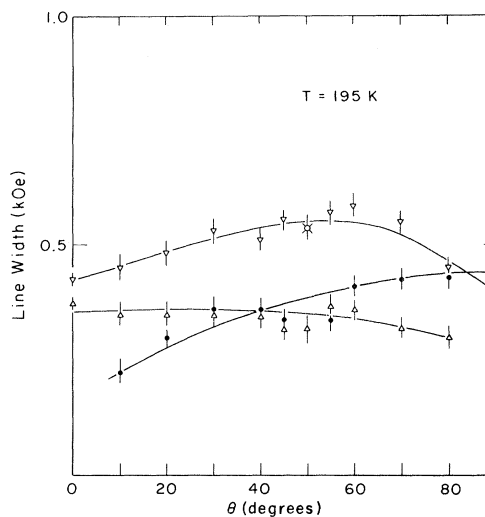


FIG. 11. Linewidth vs θ in $\text{NiSnCl}_6 \cdot 6\text{H}_2\text{O}$ for $T=195$ K.

273 K, respectively. At 4.2 K pronounced broadening occurs in the vicinity of $\theta=30^\circ$. As seen in Fig. 3 this is the angle at which the two W_{0-} transitions merge together. At 273 K the broadening occurs at $\theta=60^\circ$, which is (see Fig. 5) approximately the angle at which the W_{0-} and W_{0+} branches cross. No pronounced broadening occurs at 195 K, even though, as seen in Fig. 6, two lines coincide at $\theta=50^\circ$. The coincidence of these lines comes from the crossing of the $W_{0-}(\Delta M_s = \pm 1)$ and $W_{-+}(\Delta M_s = \pm 2)$ branches. Because of the different selection rules the probability of energy transfer

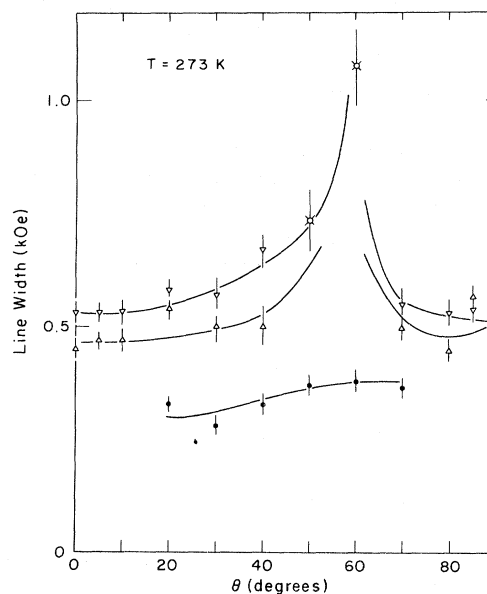


FIG. 12. Linewidth vs θ in $\text{NiSnCl}_6 \cdot 6\text{H}_2\text{O}$ for $T=273$ K.

between the two transitions is considerably reduced, with a consequent reduction in the cross-relaxation broadening.

IV. SUMMARY

The ESR measurements described in this paper support the conclusions of the low-temperature thermal and magnetic measurements that the $\text{Ni}\cdot 6\text{H}_2\text{O}^{++}$ complex in nickel chlorostannate is a system with $S=1$ in an axial crystal field $D>0$ such that the ground state is a singlet. The low-temperature value of $D=0.458\text{ cm}^{-1}$ is in good agreement with the magnetic and thermal experiments, and the temperature dependence of D is very similar to that obtained in nickel fluosilicate. We have demonstrated that in the chlorostannate

$D=0$ at 338 K; this is the first such nickel salt in which D can be made to vanish by changes of temperature alone.

The linewidth measurements indicate a variety of contributions: dipolar, isotropic exchange, anisotropic exchange, spin-lattice relaxation, and cross relaxation under certain conditions. There is clear evidence that the linewidth contribution from isotropic exchange vanishes as $D\rightarrow 0$, but that cross relaxation becomes important as the isotropic exchange contribution vanishes.

ACKNOWLEDGMENT

We should like to thank B. E. Myers for assistance with the preparation of the single-crystal samples.

*Present address: Department of Chemistry, Kyoto University, Kyoto, Japan.

†Work supported by grants from the National Science Foundation and from the Office of Naval Research. A preliminary version appears in abstract form in Bull. Am. Phys. Soc. 17, 262 (1972).

¹B. E. Myers, L. G. Polgar, and S. A. Friedberg, Phys. Rev. B 6, 3488 (1972).

²A. Abragam and M. H. L. Pryce, Proc. R. Soc. A 205, 135 (1950).

³C. Kittel, Physica (Utr.) Suppl. 24, 588 (1958).

⁴W. P. Wolf, Phys. Rev. 115, 1196 (1959).

⁵T. Moriya, Phys. Rev. 117, 635 (1960).

⁶T. Tsuneto and T. Murao, Physica (Utr.) 51, 186 (1971).

⁷L. Pauling, Z. Kristallogr. 72, 452 (1930).

⁸J. Becquerel and J. van den Handel, Physica (Utr.) 6, 1034 (1939).

⁹J. Becquerel and W. Opechowski, Physica (Utr.) 6, 1039 (1939).

¹⁰R. P. Penrose and K. W. H. Stevens, Proc. Phys. Soc. Lond. A 63, 29 (1950).

¹¹B. D. Bhattacharya and M. Majumdar, Indian J. Phys. 40, 549 (1966).

¹²J. P. Gordon, Rev. Sci. Instrum. 32, 658 (1961).

¹³M. S. de Groot and J. H. van der Waals, Mol. Phys. 3, 190 (1960).

¹⁴I. J. Fritz and Leonard Yarmus, J. Chem. Phys. 51, 1428 (1969).

¹⁵A. Abragam and B. Bleaney, *Electronic Paramagnetic Resonance of Transition Ions* (Clarendon, Oxford, England, 1970), pp. 562–564.

¹⁶M. H. L. Pryce, G. Agnetta, T. Garofano, M. B. Palma-Vittorelli, and M. U. Palma, Philos. Mag. 10, 477 (1964).

¹⁷E. Ishiguro, K. Kambe, and T. Usui, Physica (Utr.) 17, 310 (1951).

¹⁸A. N. Holden, C. Kittel, and W. A. Yager, Phys. Rev. 75, 1443 (1949).

¹⁹I. Svare and G. Seidel, Phys. Rev. 134, A172 (1964).

²⁰W. M. Walsh, Jr., Phys. Rev. 114, 1473 (1959).

²¹N. Bloembergen, S. Shapiro, P. S. Pershan, and J. O. Artman, Phys. Rev. 114, 445 (1959).